

# Unoccupied electronic states of $\text{LaCoO}_3$ and $\text{PrCoO}_3$ investigated using inverse photoemission spectroscopy and GGA+ $U$ calculations

S. K. Pandey

UGC-DAE Consortium for Scientific Research, Khandwa Road, Indore 452001, India

Ashwani Kumar

Department of Physics, Institute of Science and Laboratory Education, IPS Academy, Indore 452012, India

S. Banik, A. K. Shukla, S. R. Barman, and A. V. Pimpale

UGC-DAE Consortium for Scientific Research, Khandwa Road, Indore 452001, India

(Received 20 November 2007; revised manuscript received 12 February 2008; published 20 March 2008)

The unoccupied electronic states of  $\text{LaCoO}_3$  and  $\text{PrCoO}_3$  are studied using room temperature inverse photoemission spectroscopy and *ab initio* GGA+ $U$  band structure calculations. A fairly good agreement between experiment and theory is obtained. The intensity of the peak just above the Fermi level is found to be very much sensitive to the hybridization of Co  $3d$  and O  $2p$  orbitals. Moreover, the band just above the Fermi level is of Co  $3d$  character with little contribution from O  $2p$  states.

DOI: [10.1103/PhysRevB.77.113104](https://doi.org/10.1103/PhysRevB.77.113104)

PACS number(s): 71.20.-b, 75.20.Hr, 71.27.+a, 79.60.Bm

Perovskite type transition metal oxides with general formula  $\text{ABO}_3$  ( $A$ =rare-earth ions and  $B$ =transition metal ions) have been of much interest for more than 50 years.<sup>1</sup> Recently, research activities have been intensified in this class of materials due to the emergence of exotic properties like charge-disproportionation, charge ordering, orbital ordering, phase separation, colossal magnetoresistance, etc.<sup>1</sup> The interplay between the on-site and inter-site Coulomb interaction, the charge transfer energy, the hybridization strength between the cation  $3d$  and oxygen  $2p$  states, and the crystal field splitting for the  $d^m p^m$  configuration of the  $\text{BO}_6$  octahedron control the ground state electronic structure and magnetic and transport properties of these perovskites.

Cobaltates with general formula  $\text{ACoO}_3$  form an interesting class of compounds in the perovskite family. The ground state of these compounds is believed to be a nonmagnetic (spin  $S=0$ ) insulator having  $\text{Co}^{3+}$  ion in the low spin configuration with fully filled Co  $t_{2g}$  orbitals. These compounds show insulator-to-metal and nonmagnetic-to-paramagnetic transitions with increase in temperature.<sup>2-6</sup> It is believed that such a transition occurs due to a thermally driven spin state transition of  $\text{Co}^{3+}$  ions.<sup>7-9</sup> To understand the electronic transport in these compounds the understanding of both the occupied and the unoccupied electronic states is desirable. Most of the work found in literature deals only with the occupied part of the electronic states.<sup>10-16</sup> There are very few reports in the literature dealing with the unoccupied electronic states and most of them are based on x-ray absorption studies of  $\text{LaCoO}_3$ .<sup>17-19</sup>

Here we study the unoccupied electronic states of  $\text{LaCoO}_3$  and  $\text{PrCoO}_3$  using inverse photoemission spectroscopy (IPES) and show how the unoccupied electronic states are affected when La is replaced by Pr. The replacement of La by Pr has a twofold effect: (i) change in chemical pressure due to changed ionic radius and (ii) change in the electronic occupancy of  $4f$  states. The change in chemical pressure may affect the crystal structure of  $\text{PrCoO}_3$ . The powder diffraction work has shown the crystal structure of  $\text{LaCoO}_3$

and  $\text{PrCoO}_3$  as rhombohedral and orthorhombic, respectively.<sup>6,20</sup> The  $\text{Pr}^{3+}$  ion contains two electrons in the  $4f$  states. This would contribute to the valence band and is expected to affect the unoccupied electronic structure of the compound.

In the present work, we investigate the room temperature unoccupied electronic structure of  $\text{LaCoO}_3$  and  $\text{PrCoO}_3$  compounds using IPES and *ab initio* band structure calculation. The comparison of experimental spectra with the convoluted total density of states indicates that GGA+ $U$  calculation is sufficient for understanding all experimentally observed features in the spectrum. On going from  $\text{LaCoO}_3$  to  $\text{PrCoO}_3$  the intensity of the peak just above the Fermi level decreases for  $\text{PrCoO}_3$  due to decrease in the hybridization of Co  $3d$  and O  $2p$  orbitals in this compound in comparison to  $\text{LaCoO}_3$ . The band just above the Fermi level is of Co  $3d$  character.

$\text{LaCoO}_3$  and  $\text{PrCoO}_3$  were prepared in the polycrystalline form by the combustion method.<sup>21</sup> Nitrates of La, Pr, and Co were taken in an appropriate amount and mixed in double distilled water. In this mixture, 2 moles of glycine per 1 mole of metal cation was added and stirred until all the compounds dissolved in the water. The resulting solution was heated slowly at temperature around 200 °C until all the water evaporated. The precursor thus formed catches fire on its own making the powder of the desired compound. The hard pellets of this powder were formed and heated at 1200 °C for 1 day. The samples were characterized by the x-ray powder diffraction technique. The powder diffraction data did not show any impurity peak; all the peaks of  $\text{LaCoO}_3$  and  $\text{PrCoO}_3$  were well-fitted with rhombohedral (space group  $R\bar{3}c$ ) and orthorhombic (space group  $Pbnm$ ) phases, respectively, using the Rietveld refinement technique. The lattice parameters obtained from the fitting agree well with those reported in the literature.<sup>20,22</sup>

The inverse photoemission spectroscopy experiments on  $\text{LaCoO}_3$  and  $\text{PrCoO}_3$  compounds were performed under ultrahigh vacuum at a base pressure of  $6 \times 10^{-11}$  mbar. The

samples were mounted in the form of a compressed hard pellet and they were scraped uniformly by a diamond file to obtain a clean surface. An electrostatically focused electron gun of Stoffel Johnson design and an acetone gas filled photon detector with a  $\text{CaF}_2$  window were used for the experiments.<sup>23,24</sup> The experiments were carried out in the isochromat mode where the kinetic energy of the incident electrons was varied at 0.05 eV steps and photons of fixed energy (9.9 eV) were detected with an overall resolution of 0.55 eV.<sup>24</sup> Fermi level was aligned by recording the IPES spectrum of *in situ* cleaned silver foil. Since the incident electron beam intensity is not constant over the studied kinetic energy range, its intensity is measured simultaneously with the photon intensity at each kinetic energy step by measuring the current through the sample. The spectra are normalized by dividing the photon intensity by the current through the sample, as in our earlier work.<sup>25</sup>

The GGA+ $U$  spin-polarized density of states (DOS) calculation of  $\text{LaCoO}_3$  was carried out using LMTART 6.61.<sup>26</sup> Here, we have used a cubic perovskite structure with lattice parameter  $a=7.2913$  a.u., which is equal to twice the Co-O bond length.<sup>20</sup> For calculating charge density, a full-potential linearized muffin-tin orbital method working in plane wave representation was employed. In the calculation, we have used the muffin-tin radii of 3.509, 2.001, and 1.674 a.u. for La, Co, and O, respectively. The charge density and effective potential were expanded in spherical harmonics up to  $l=6$  inside the sphere and in a Fourier series in the interstitial region. The initial basis set included  $6s$ ,  $6p$ ,  $5d$ , and  $4f$  valence, and  $5s$  and  $5p$  semicore orbitals of La;  $4s$ ,  $4p$ , and  $3d$  valence, and  $3p$  semicore orbitals of Co, and  $2s$  and  $2p$  valence orbitals of O. The exchange correlation functional of the density functional theory was taken after Vosko *et al.*<sup>27</sup> and generalized gradient approximation (GGA) was implemented using the Perdew *et al.* prescription.<sup>28</sup> In the GGA+ $U$  calculations the Hubbard  $U$  and exchange  $J$  are considered as parameters. We have taken  $U=3.5$  eV and  $J=1.0$  eV for Co  $3d$  electrons. The values of  $U$  and  $J$  for  $3d$  electrons are consistent with our previous studies.<sup>13,15</sup> Self-consistency was achieved by demanding the convergence of the total energy to be smaller than  $10^{-5}$  Ryd/cell. The final self-consistent solution converged to a low spin state. (6, 6, 6) divisions of the Brillouin zone along three directions for the tetrahedron integration were used to calculate the density of states (DOS). To calculate the IPES spectrum, the unoccupied partial DOS thus obtained were first convoluted with an energy dependent Lorentzian [full width at half maximum (FWHM)= $0.1(E-E_F)$  eV] to account for the lifetime broadening and a Gaussian having a FWHM of 0.55 eV to account for resolution broadening and then a parabolic background was added.

The experimental spectra of  $\text{LaCoO}_3$  and  $\text{PrCoO}_3$  are plotted in Fig. 1. The normalized spectra of these compounds in the region closer to the Fermi level are given in the inset of the figure. Three features are clearly seen in the spectrum corresponding to  $\text{LaCoO}_3$  denoted by A, B, and C. Peaks B and C are not separately observed in  $\text{PrCoO}_3$ , rather a broad peak is observed centered around 7 eV. It may be noted that the first peak A is somewhat more asymmetric for  $\text{LaCoO}_3$  as compared to  $\text{PrCoO}_3$ . This may be an indication of some

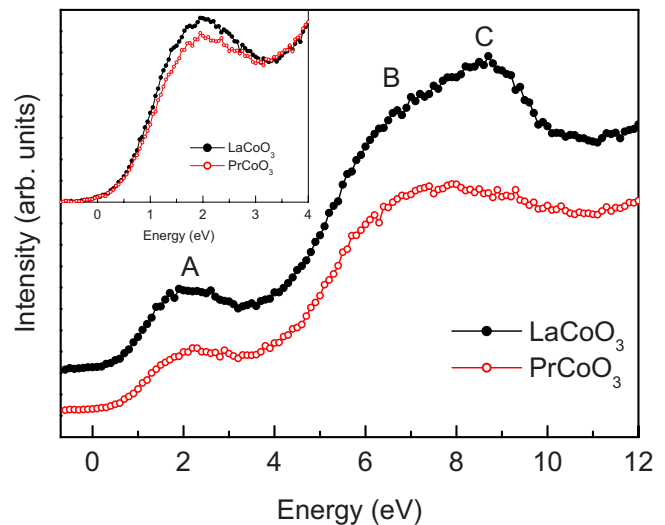


FIG. 1. (Color online) Inverse photoemission spectra of  $\text{LaCoO}_3$  and  $\text{PrCoO}_3$ . The inset shows the normalized spectra near the Fermi level of these compounds. The energy origin is taken at the Fermi level.

additional structure around this energy in  $\text{LaCoO}_3$ . The feature B is not seen in the bremsstrahlung isochromat spectroscopy (BIS) data of  $\text{LaCoO}_3$  of Chainani *et al.*<sup>18</sup> This may be due to different cross section and lower resolution of the BIS data. It is clear from the inset that there is little intensity near the Fermi level, indicating the insulating nature of the compounds. The rise in the intensity above the Fermi level is relatively sharper for  $\text{LaCoO}_3$  in comparison to  $\text{PrCoO}_3$ . Also the height of peak A corresponding to  $\text{PrCoO}_3$  is less in comparison to that in  $\text{LaCoO}_3$ .

The experimental and calculated IPES spectra of  $\text{LaCoO}_3$  are plotted in Fig. 2. The cross section of the La  $4f$  states relative to the La  $5d$  states is taken to be similar to that of La metal. From the IPES spectrum of La reported by Duo and co-workers,<sup>29</sup> we find the cross-section of La  $4f$  to be 10% of the cross section of La  $5d$  at 10.2 eV photon energy. A similar  $4f$  to  $5d$  ratio has also been obtained for Gd.<sup>30</sup> Thus the

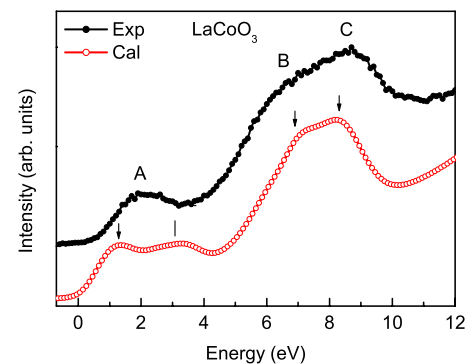


FIG. 2. (Color online) The experimental and calculated inverse photoemission spectra of  $\text{LaCoO}_3$ . The calculated spectrum is obtained by convoluting the total unoccupied DOS first with a Lorentzian and then by a Gaussian; an energy dependent parabolic background is also added to the theoretical spectrum.

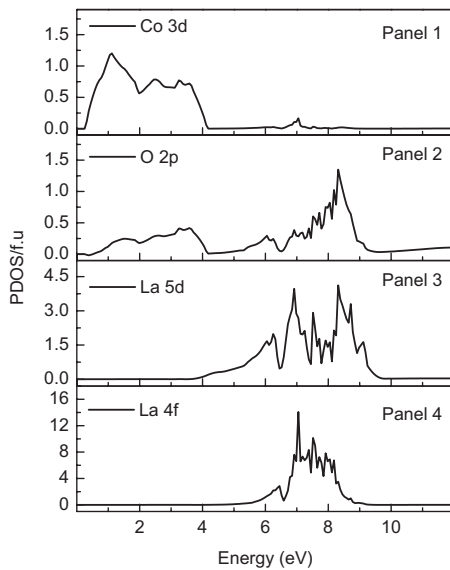


FIG. 3. Partial density of states of Co  $3d$ , O  $2p$ , La  $5d$ , and La  $4f$  characters for LaCoO<sub>3</sub>.

calculated IPES spectrum in Fig. 2 is obtained by adding broadened partial DOS of Co  $3d$ , O  $2p$ , and La  $5d$  with  $0.1 \times$  La  $4f$ . Furthermore, a parabolic inelastic background is also added. The IPES spectrum calculated in this way exhibits good agreement with the experiment. It contains three features denoted by arrows corresponding to the experimentally observed features A, B, and C. In addition, a structure is seen around 3 eV (shown by tick), which may account for the asymmetry of peak A in the experimental data. There is some deviation in the energy positions and the corresponding intensities of the features. Such deviation may be due to approximations in the DOS calculation and cross sections.

To identify the contributions of the different partial DOS in the different features in the experimental LaCoO<sub>3</sub> spectrum, we have plotted the Co  $3d$ , O  $2p$ , La  $5d$ , and La  $4f$  partial DOS in Fig. 3, as these DOS contribute most in the energy regions of interest. It is evident from panels 1 and 2 that in feature A, Co  $3d$  and O  $2p$  states contribute. There is a substantial rise in Co  $3d$  DOS just above the Fermi level indicating that the region just above it has only Co  $3d$  character. Feature B mainly arises from electronic transition to La  $5d$  states with a small contribution from La  $4f$  states. Feature C can be attributed primarily to La  $5d$  and O  $2p$  states

with a small contribution from La  $4f$  states. It is evident from panels 2, 3, and 4 that the La  $4f$  partial DOS is much larger than the O  $2p$  and La  $5d$  partial DOS, but it hardly contributes to the spectral shape due to its smaller cross section, as discussed earlier.

The reduced asymmetry and intensity under peak A for PrCoO<sub>3</sub> can be seen to be due to unoccupied O  $2p$  DOS. It may be noted that the overlap of Co  $3d$  and O  $2p$  orbitals is somewhat reduced for the PrCoO<sub>3</sub> in comparison to LaCoO<sub>3</sub> due to increased average Co-O bond length as revealed by our extended x-ray absorption fine structure (EXAFS) studies.<sup>31</sup> The decrease in overlap will reduce the transfer of electron from the O  $2p$  to Co  $3d$  orbital and as a consequence decrease in the unoccupied O  $2p$  band. The interpretation is in line with the plotted partial DOS in panel 2 of Fig. 3 where O  $2p$  DOS contributing to these features is 1 eV above the Fermi level from where the intensity started decreasing for PrCoO<sub>3</sub>, as is evident from Fig. 1. This behavior of intensity clearly indicates that the band just above the Fermi level is of  $d$  character arising from Co  $3d$  partial DOS. This result is in contrast with configuration interaction calculations of Saitoh *et al.*<sup>32</sup> giving O  $2p$  character of band just above the Fermi level for LaCoO<sub>3</sub>. Here, it is important to note that the occupied electronic structure of cobaltates is seen to be very much sensitive to the spin state of the Co ions, whereas the unoccupied states just above the Fermi level are almost insensitive.<sup>9,15,16,33</sup> Therefore the band just above the Fermi level would be predominantly of Co  $3d$  character irrespective of the spin state of Co ions.

In conclusion, we have carried out room temperature inverse photoemission spectroscopy (IPES) measurements on LaCoO<sub>3</sub> and PrCoO<sub>3</sub> compounds. The IPES data are analyzed by using density of states obtained from GGA+ $U$  calculations. It is noted that such calculations might suffice to understand the features observed in the experimental spectra up to 12 eV above the Fermi level. The hybridization of Co  $3d$  and O  $2p$  orbitals is found to be crucial for understanding the change in intensity of the peak just above the Fermi level. The band just above it is of Co  $3d$  character with little contribution from O  $2p$  states.

B. A. Dasannacharya, P. Chaddah, A. Gupta, and K. Horn are thanked for constant encouragement. Financial support from Department of Science and Technology, Government of India through Project No. SP/S2/M-06/99, Ramanna research grant, and Max-Planck Partner group project is gratefully acknowledged.

<sup>1</sup>M. Imada, A. Fujimori, and Y. Tokura, Rev. Mod. Phys. **70**, 1039 (1998).

<sup>2</sup>R. R. Heikes, R. C. Miller, and R. Mazelsky, Physica (Amsterdam) **30**, 1600 (1964).

<sup>3</sup>V. G. Bhide, D. S. Rajoria, and Y. S. Reddy, Phys. Rev. Lett. **28**, 1133 (1972).

<sup>4</sup>S. Yamaguchi, Y. Okimoto, and Y. Tokura, Phys. Rev. B **54**, R11022 (1996).

<sup>5</sup>S. Yamaguchi, Y. Okimoto, H. Taniguchi, and Y. Tokura, Phys. Rev. B **53**, R2926 (1996).

<sup>6</sup>S. Tsubouchi, T. Kyômen, M. Itoh, and M. Oguni, Phys. Rev. B **69**, 144406 (2004).

<sup>7</sup>J. B. Goodenough, J. Phys. Chem. Solids **6**, 287 (1958).

<sup>8</sup>P. M. Raccach and J. B. Goodenough, Phys. Rev. **155**, 932 (1967).

<sup>9</sup>M. A. Korotin, S. Yu. Ezhov, I. V. Solovyev, V. I. Anisimov, D. I. Khomskii, and G. A. Sawatzky, Phys. Rev. B **54**, 5309 (1996).

- <sup>10</sup>D. J. Lam, B. W. Veal, and D. E. Ellis, *Phys. Rev. B* **22**, 5730 (1980).
- <sup>11</sup>S. R. Barman and D. D. Sarma, *Phys. Rev. B* **49**, 13979 (1994).
- <sup>12</sup>T. Saitoh, T. Mizokawa, A. Fujimori, M. Abbate, Y. Takeda, and M. Takano, *Phys. Rev. B* **55**, 4257 (1997).
- <sup>13</sup>S. K. Pandey, A. Kumar, S. M. Chaudhari, and A. V. Pimpale, *J. Phys.: Condens. Matter* **18**, 1313 (2006).
- <sup>14</sup>T. Saitoh, D. Ishii, A. Hachimura, M. Hirose, T. S. Naing, Y. Kobayashi, K. Asai, M. Nakatake, M. Higashiguchi, K. Shimada, H. Namatame, and M. Taniguchi, *J. Magn. Magn. Mater.* **310**, 981 (2007).
- <sup>15</sup>S. K. Pandey, A. Kumar, S. Patil, V. R. R. Medicherla, R. S. Singh, K. Maiti, D. Prabhakaran, A. T. Boothroyd, and A. V. Pimpale, *Phys. Rev. B* **77**, 045123 (2008).
- <sup>16</sup>S. K. Pandey, S. Patil, V. R. R. Medicherla, R. S. Singh, and K. Maiti, arXiv:0711.1020v1.
- <sup>17</sup>M. Abbate, J. C. Fuggle, A. Fujimori, L. H. Tjeng, C. T. Chen, R. Potze, G. A. Sawatzky, H. Eisaki, and S. Uchida, *Phys. Rev. B* **47**, 16124 (1993).
- <sup>18</sup>A. Chainani, M. Mathew, and D. D. Sarma, *Phys. Rev. B* **46**, 9976 (1992).
- <sup>19</sup>S. K. Pandey, A. Kumar, S. Khalid, and A. V. Pimpale, *J. Phys.: Condens. Matter* **18**, 7103 (2006).
- <sup>20</sup>P. G. Radaelli and S. W. Cheong, *Phys. Rev. B* **66**, 094408 (2002).
- <sup>21</sup>S. K. Pandey, R. Bindu, P. Bhatt, S. M. Chaudhari, and A. V. Pimpale, *Physica B* **365**, 47 (2005).
- <sup>22</sup>K. Yoshii, S. Tsutsui, and A. Nakamura, *J. Magn. Magn. Mater.* **226-230**, 829 (2001).
- <sup>23</sup>D. Funnemann and H. Merz, *J. Phys. E* **19**, 554 (1985).
- <sup>24</sup>S. Banik, A. K. Shukla, and S. R. Barman, *Rev. Sci. Instrum.* **76**, 066102 (2005); A. K. Shukla, S. Banik, and S. R. Barman, *Curr. Sci.* **90**, 490 (2006).
- <sup>25</sup>S. Banik, A. Chakrabarti, U. Kumar, P. K. Mukhopadhyay, A. M. Awasthi, R. Ranjan, J. Schneider, B. L. Ahuja, and S. R. Barman, *Phys. Rev. B* **74**, 085110 (2006).
- <sup>26</sup>S. Y. Savrasov, *Phys. Rev. B* **54**, 16470 (1996); S. Y. Savrasov, arXiv:cond-mat/0409705v1, *J. Comput. Crystallogr.* (to be published).
- <sup>27</sup>S. H. Vosko, L. Wilk, and M. Nusair, *Can. J. Phys.* **58**, 1200 (1980).
- <sup>28</sup>J. P. Perdew, K. Burke, and M. Ernzerhof, *Phys. Rev. Lett.* **77**, 3865 (1996).
- <sup>29</sup>L. Duò, M. Finazzi, and L. Braicovich, *Phys. Rev. B* **48**, 10728 (1993).
- <sup>30</sup>Th. Fauster and F. J. Himpsel, *Phys. Rev. B* **30**, 1874 (1984).
- <sup>31</sup>S. K. Pandey, S. Khalid, N. P. Lalla, and A. V. Pimpale, *J. Phys.: Condens. Matter* **18**, 10617 (2006).
- <sup>32</sup>T. Saitoh, A. E. Bocquet, T. Mizokawa, and A. Fujimori, *Phys. Rev. B* **52**, 7934 (1995).
- <sup>33</sup>K. Knížek, Z. Jiráček, J. Hejtmánek, and P. Novák, *J. Phys.: Condens. Matter* **18**, 3285 (2006).